Available online at www.sciencedirect.com
SCIENCE DIRECT
Polymer 46 (2005) 10113–10118
polymer
www.elsevier.com/locate/polymer

A block copolymer nanotemplate for mechanically tunable polarized emission from a conjugated polymer

Tao Deng[a,b], Craig Breen[a,c], Thomas Breiner[b], Timothy M. Swager[a,c], Edwin L. Thomas[a,b,*]

[a]*Institute for Soldier Nanotechnologies, Massachusetts Institute of Technology, Building NE47, 4th Floor, Room 13-5094, 77 Massachusetts Avenue, Cambridge, MA 02139, USA*
[b]*Department of Materials Science and Engineering, Massachusetts Institute of Technology, 77 Massachusetts Avenue, Cambridge, MA 02139, USA*
[c]*Department of Chemistry, Massachusetts Institute of Technology, 77 Massachusetts Avenue, Cambridge, MA 02139, USA*

Received 29 August 2004; received in revised form 28 April 2005; accepted 17 August 2005
Available online 8 September 2005

Abstract

A polymer blend system consisting of polystyrene grafted onto poly (*p*-phenylene ethynylene) (PS-*g*-PPE) and poly (styrene-*block*-isoprene-*block*-styrene) triblock copolymer (SIS) yields highly polarized emission due to the unidirectional alignment of the PPE molecules. During the roll casting, the triblock copolymer microphase separates and creates unidirectionally aligned PS cylindrical microdomains in the rubbery PI matrix. PPE, a fluorescent conjugated polymer, was grafted with polystyrene (PS) side chains that enabled sequestration and alignment of these rigid backbone emitter molecules into the PS microdomains of the SIS triblock copolymer. Deforming the thermoplastic elastomer in a direction perpendicular to the orientation direction of the cylinders causes rotation of the PS cylinders and the PPE emitter molecules and affords tunable polarized emission due to re-orientation of the PPE containing PS cylinders as well as film thinning from Poisson effect.

Keywords: Block copolymer; Template; Polarized emission

1. Introduction

Block polymers are comprised of two or more chemically distinct blocks that are covalently linked into polymer chains. When the different blocks have a strongly repulsive interaction, they tend to microphase separate into microdomains to minimize the overall free energy. Typically the interaction between different blocks varies inversely with temperature, so cooling a block copolymer from its high temperature homogeneous melt to below its order to disorder transition (ODT) results in microphase separation. Alternatively the repulsive interaction between the blocks can be screened by solvent. In this case, solvent evaporation increases the effective interaction, and induces microphase separation once the system crosses the order to disorder concentration. Microphase-separated block copolymers can form numerous morphologies depending on their composition. The simplest linear AB diblock copolymers, for example, form sphere, cylinder, double gyroid, and lamellar morphologies. Some complex block copolymers, e.g. miktoarm star terpolymers, show many other morphologies [1]. In all these morphologies, block copolymer microdomains self assemble into one-, two-, and three-dimensional periodically ordered structures. In 1971, Keller et al. demonstrated near single crystal texture development in an ABA triblock copolymer using the flow field generated in a capillary rheometer [2]. This discovery stirred interest in the global ordering of block copolymer microdomains and various methods have been developed over the last several decades [3–6]. A roll casting process for ordering block copolymer microdomains from a solution was developed using the flow field generated between two counter rotating rollers [4]. It offers a convenient alternative route to large area ordered block copolymer microdomain films without involving strong electric field and/or high temperature processing. Roll casting is also a process that is

* Corresponding author. Address: Institute for Soldier Nanotechnologies, Massachusetts Institute of Technology, Building NE47, 4th Floor, Room 13-5094, 77 Massachusetts Avenue, Cambridge, MA 02139, USA. Tel.: +1 617 253 5931; fax: +1 617 253 5859.
E-mail address: elt@mit.edu (E.L. Thomas).

0032-3861/$ - see front matter © 2005 Elsevier Ltd. All rights reserved.
doi:10.1016/j.polymer.2005.08.060

amenable to large-scale production and to high molecular weight polymers where the ODT is well above the thermal degradation temperature.

Highly organized block copolymers offer many opportunities for applications requiring such order for systematic control and precise property manipulation [7–10]. For example, Ha et al. systematically studied a block copolymer-layered silicate nanocomposite system in which the block copolymer microdomains were ordered by roll-casting [7,11]. Li et al. used block copolymer templates to fabricate ordered GaAs nanostructures [8]. Cheng et al. have used a block copolymer combined with graphoepitaxy to produce a 2D mask for creation of ultrahigh density 2D cobalt dot arrays as magnetic storage media [9]. The use of block polymers as a directing template for nanoparticles is very analogous to the situation in this paper where instead of a nanoparticle, the block copolymer is used to both guide emitter molecules into specific domains and to create alignment of these guest molecules [12]. The role of block copolymers in a host of nanotechnology related applications has been recently reviewed [13].

Polymers offer a versatile matrix to host optically active molecules. For example, polarized emission from a dopant has previously been reported in stretched polymer films [14,15]. Gin et al. reported a self-assembly approach in templating poly(phenylenevinylene) (PPV) into hexagonally ordered microdomain structures [16]. In their approach, however, only a very low concentration of PPV could be loaded in the template, so no polarized light emission data could be measured since their system was not well ordered over a large region necessary for generating sufficient polarized emission. Recently we demonstrated a self-assembly approach to template a conjugated light emitting PPE polymer within a SIS triblock copolymer nanotemplate for the generation of polarized emission [17]. By co-assembly of the block copolymer and the PS-*g*-PPE emitters in a roll cast process, the PPE molecules were sequestered inside the PS microdomains and the PS cylindrical microdomains were aligned by the flow field. In this paper, we prepared a series of roll-cast SIS-PS-*g*-PPE thin films with various thicknesses and characterize them using transmission electron microscopy (TEM), small angle X-ray scattering (SAXS), and fluorescence spectroscopy. We compare the emission properties of this highly anisotropic system with those of the corresponding simple cast isotropic SIS-PS-*g*-PPE system. We also present an initial study of the strain dependence of the polarized emission for samples deformed perpendicular to the orientation direction of the anisotropic film.

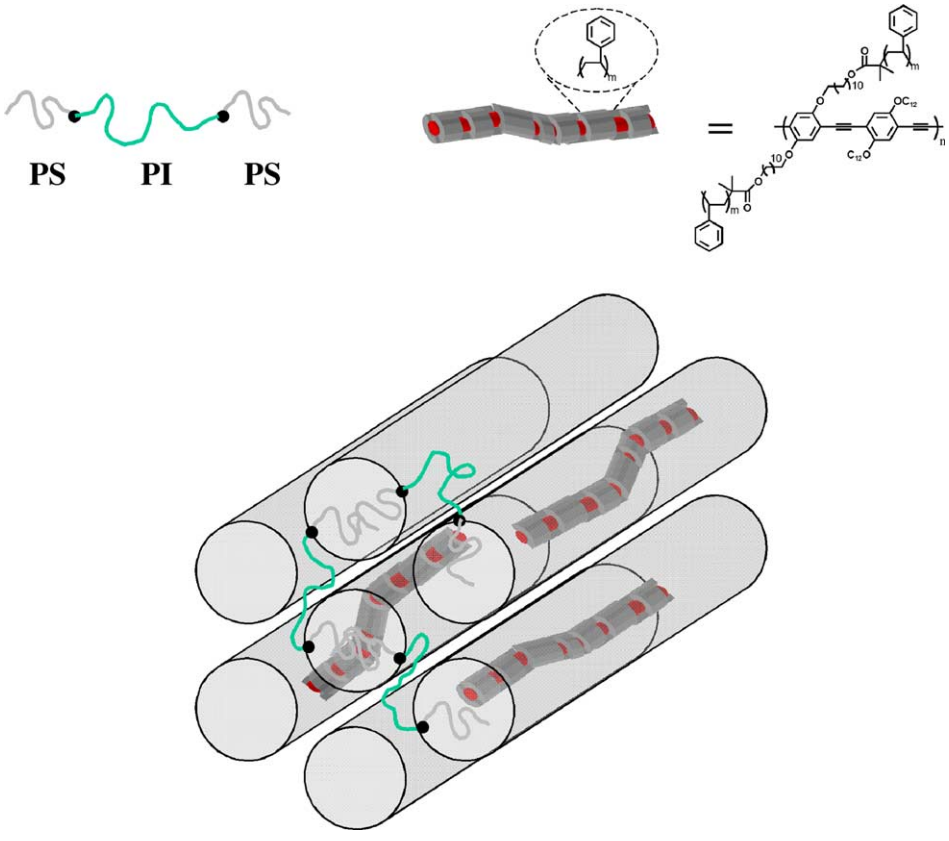

Fig. 1. Schematic showing the alignment of PS-*g*-PPE by sequestration inside the PS domains of a SIS triblock copolymer. PPE was grafted with PS side chains and co-assembled into PS cylinders within the PI matrix. After the ATRP grafting reaction there are both PS side chains and hexadecane side chains on the PPE backbone.

2. Results and discussion

Poly(styrene-*block*-isoprene-*block*-styrene) triblock copolymer was obtained from Dexco (Dexco Polymers, 12012 Wickchester, Houston, TX 77079). The triblock has a composition of 29 wt% PS (26 vol%), a total molecular weight of 1.01×10^5 g/mol and a polydispersity of 1.05. The PS block forms cylindrical microdomains in the PI matrix upon microphase separation. The intercylinder spacing is ~31 nm, and the diameter of cylinders is ~8 nm [18,19]. PPE with grafted PS side chains was synthesized by grafting styrene from a PPE macroinitiator via atom transfer radical polymerization (ATRP) [17]. The average molecular weight of PPE backbone is $\sim5.6\times10^4$ g/mol and that of the styrene grafted PPE increases to $\sim8.0\times10^4$ g/mol. The PS grafts were cleaved off the PPE backbone and their average molecular weight was determined as 5600 g/mol. The end-to-end distance of a PS homopolymer with a molecular weight of 5600 g/mol is about 5 nm and the average contour length of a PPE emitter molecule is about 30 nm. The persistence length of similar PPEs was measured to be 15 nm [20], so the PS-*g*-PPE component can be pictured as a reasonably stiff, 30 nm long PS coated 5 nm diameter particle with an aspect ratio of roughly 3.

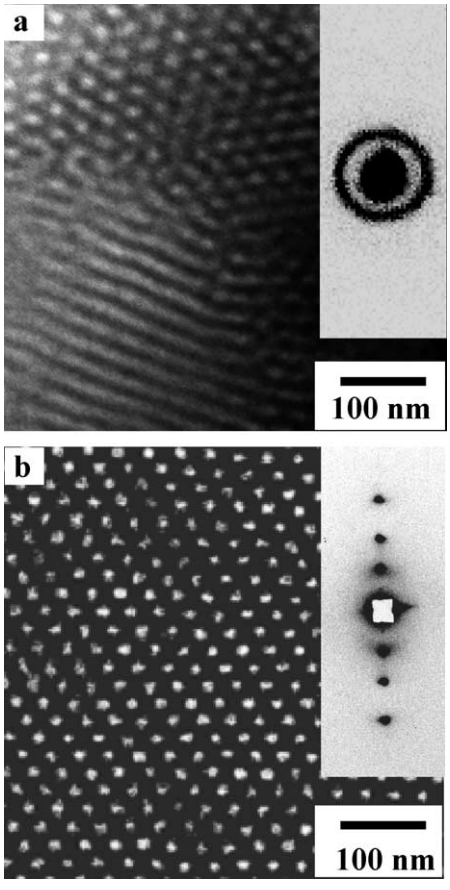

Fig. 2. Cross-sectional transmission electron microscopy (TEM) images and small angle X-ray scattering (SAXS) data. (a) SIS triblock copolymer blended with 0.1% (w/w) PS-*g*-PPE after simple casting. Small grains and a lack of overall microdomain ordering are apparent in the TEM image and an isotropic scattering ring is evident in the SAXS pattern. (b) Same system after roll casting. The TEM view is along the axis of the cylinders showing the PS cylinders (white circular dots) form a long-range ordered hexagonal lattice in the PI matrix. The SAXS pattern with the incident X-ray beam orthogonal to the cylinders shows the $\sqrt{1}$, $\sqrt{3}$, and $\sqrt{4}$ reflections of the hexagonal lattice of cylinders. The FWHM of the first reflection is only 10°, indicating the high axial alignment achieved by the roll cast process.

Oriented co-assembled films of SIS/PS-*g*-PPE were prepared by roll casting [4]. Two independent motors control two parallel rollers, one of stainless steel and the other of teflon. A micrometer controls the gap between the rollers. Adding a concentrated solution of polymer into the gap region uniformly coats both rollers. The gap and roller speeds are set to typical values of 0.04–0.5 mm and 15 rpm, respectively. During roll casting, the roll caster was covered with a box to slow the evaporation of solvent. Cumene, like toluene, has been found to be a nonpreferential solvent for the styrene–isoprene system with the additional property of having a lower vapor pressure. Slower solvent evaporation leads to an extended period of orienting during film formation. To prepare the roll casting solution, we added a solution of 0.05% (w/w) PS-*g*-PPE in tetrahydrofuran (THF) into a solution of 40% SIS in cumene. In the combined solution, the emitter was about 0.1% (w/w) of SIS. Once the two solutions were uniformly mixed, the combined solution was exposed to air for several hours. Most THF was evaporated during this period since it has a much higher vapor pressure than cumene. A final solution of approximately 40% (w/w) of SIS/PS-*g*-PPE in cumene was roll cast. After roll casting, the film was dried overnight before removal from the rollers (Fig. 1).

Simple cast films were prepared by quiescently casting on glass slides using the same solution as for the roll casting. During simple casting, glass slides were also covered with a box to slow solvent evaporation. Structural characterization of the guest/host films was done by TEM and SAXS. Fig. 2 shows the TEM images and the corresponding SAXS patterns of both simple cast and roll cast films. To prepare the TEM sample, a small piece of polymer was embedded in epoxy and then microtomed using a Reichert–Jung Ultracut FC 4E at temperatures of −90 (knife) and −110 °C (sample) with a nominal section thickness of 70 nm. The sections were subsequently placed above a 4% aqueous solution of osmium tetraoxide for 2 h to selectively stain the PI block. A thin carbon film was also evaporated onto the sections to enhance electrical conductivity before performing TEM. TEM was carried out on a JEOL 200 CX using a tungsten filament source at 200 keV accelerating voltage. SAXS studies were performed at the Cornell High Energy Synchrotron Source (CHESS) using monochromatic X-rays and a 2D charge coupled detector (CCD). The selected X-ray wavelength was 1.51 Å while the sample to detector distance was 250 cm.

A TEM image of the simple cast film is presented in Fig. 2(a) and (b) shows a TEM image of the roll cast film with the viewing direction along the cylinder axis. After

microphase separation, the PS cylinders in the simple cast films arrange into small grains as evidenced in Fig. 2(a), whereas in roll cast films, the PS cylinders formed a hexagonal lattice in PI matrix with excellent long range order. The SAXS patterns also demonstrate the isotropic, polygranular nature of the simple cast films via the presence of uniform scattering rings (Fig. 2(a) insert). The long-range order of the PS cylinders in the roll cast films is evidenced by the near single crystal texture of the SAXS patterns (Fig. 2(b) insert). The azimuthal full-width at half-maximum (FWHM) of the $(10\bar{1}0)$ reflection of the roll cast film (the first peak in Fig. 2(b) insert) is approximately 10°. In roll cast films, the flow field generated induces the alignment of the PS cylinders along the flow direction. Optical characterization (see below) demonstrates that the PS grafted PPE molecules also align along the flow direction.

Fig. 3(a) and (b) are the polarized emission spectra of a simple cast film and a roll cast film. Both films had a thickness of ~40 μm. Spectra were collected using a SPEX Fluorolog-τ2 fluorometer (model FL112, 450 W xenon lamp) equipped with a 1935B polarization kit. In characterizing the roll cast films, the optical measurements were done by aligning the excitation polarizer with the PS cylinder axis direction. The emission polarizer is then aligned either parallel to the excitation polarizer ($I_{\parallel}$) or perpendicular to the excitation polarizer ($I_{\perp}$). Before each measurement, the spectrometer was calibrated using a standard aqueous silica bead solution (Dupont, Ludox). Fig. 3(a) shows that as expected, the simple cast film does not exhibit polarized emission. The roll cast film (Fig. 3(b)) displays polarized emission with polarization ratio ($I_{\parallel}/I_{\perp}$) about 6.2. In the roll cast films the PS grafted PPE molecules have a preferential alignment along the PS cylinder axis.

Fig. 4 shows the angular dependence of anisotropy in a simple cast film and a roll cast film (both measured at the peak position of the emitted radiation, i.e. at 472 nm). The films were mounted on a rotation stage and rotated to specific angles before each measurement. The angle between the excitation polarizer and the cylinder axis is designated as θ. The anisotropy r of the emitting light is defined as [21]:

$$r(\theta) = \frac{(I_{\parallel}(\theta) - I_{\perp}(\theta))}{(I_{\parallel}(\theta) + 2I_{\perp}(\theta))}$$

For the simple cast film, since the cylinders have no overall orientational anisotropy, neither do the conjugated emitter molecules. Consequently the anisotropy does not change with angle as shown in Fig. 4. In the roll cast films, the anisotropy is maximum when $\theta = 0°$ (the excitation polarizer is parallel to the cylinder axis), and minimum for $\theta = 90°$. For an ideally ordered guest/host film without scattering and other depolarization effects, the anisotropy will be proportional to $\cos^2(\theta)$ [22]. The solid line in Fig. 4 is a fit to $r = (r_{max} - r_{min})\cos^2(\theta) + r_{min}$, in which r_{max} is the

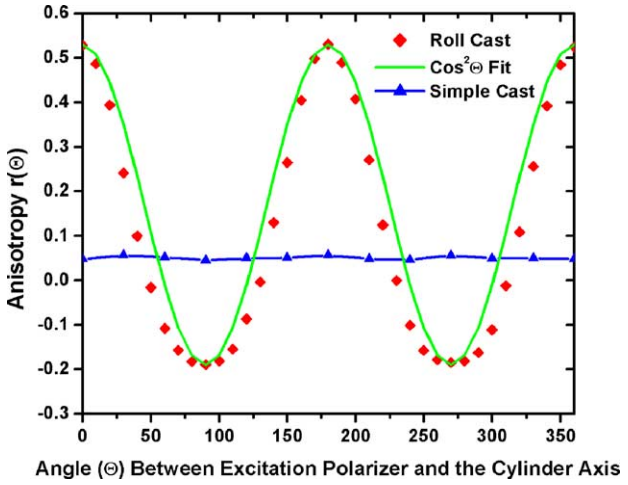

Fig. 4. Angular dependence of anisotropy $r(\theta)$ of a simple cast film and a roll cast film at 472 nm. The thickness of both films was ~80 μm. The nonzero anisotropy in the isotropic film arises due to the polarized excitation.

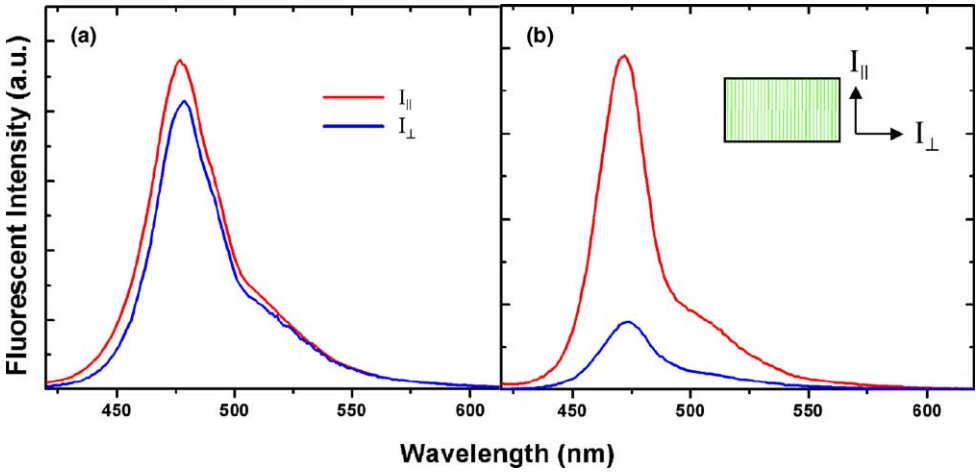

Fig. 3. Emission spectrum of (a) a simple cast film and (b) a roll cast film. The thickness of both films was ~40 μm. The excitation wavelength was ~400 nm and the sample was irradiated perpendicular to the surface of the film.

maximum experimental anisotropy and r_{min} is the minimum. The experimentally observed anisotropy values are smaller than the theoretical values based on perfect alignment. One way the anisotropy can decrease is due to depolarization of the emitted light by scattering within the sample. In order to understand origins of depolarization, we studied the thickness dependence of the polarized emission in roll cast films by roll casting films with thickness in the range of 0.04–0.5 mm. The FWHM of the $(10\bar{1}0)$ reflection of all these films is in the range of 10–12° so we can assume any decrease in the anisotropy is not due to alignment differences of the PS cylinders. Fig. 5 shows the anisotropy (at 472 nm) of these films with different thicknesses. The decrease in anisotropy with the increase in film thickness suggests that depolarization is mainly due to the scattering inside the polymer films. In a single scattering event, the anisotropy could decrease to 70% of its original value [22]. As the thickness of the film increases, the scattering increases and the anisotropy decreases. If scattering is the only mechanism for depolarization, then we should expect the anisotropy to decrease linearly with the increase of sample thickness [22], which is in reasonable agreement with the data in Fig. 5. The picture that emerges is that the PS cylinders are better aligned than the much smaller aspect ratio PS-*g*-PPE 'particles' inside them (Fig. 1).

This SIS-PS-*g*-PPE system not only has emission anisotropy, but also has mechanical anisotropy [18,19]. The film is strong and stiff along the PS cylinder direction while it is soft and easily deformed normal to cylinder direction. This mechanical anisotropy is simply due to the parallel and serial arrangements of the glassy PS cylinders in the rubbery PI matrix, respectively, for loading along the two orthogonal directions. As force is applied normal to the cylinder axis, the PS cylinders initially move apart and then eventually kink bands are initiated and the cylinders rotate towards the stretch direction. At short times after the release of force, the cylinders do not fully recover to their original alignment and there is residual strain in the system. During the second (and subsequent) loading/unloading cycle, however, the cylinders approximately recover to their initial state at the beginning of the second cycle, and the film shows nearly reversible deformation behavior. Fig. 6 shows the measured optical anisotropy as a function of applied strain for the second loading and unloading cycle. When force is applied normal to the original roll cast direction, the film thickness decreases and above some strain, the PS cylinders buckle and rotate towards the stretching direction. Consequently, the normalized optical anisotropy decreases, dropping by about 50% of the initial normalized anisotropy at a strain of about 200%. After releasing the force, the rubbery PI matrix pulls the PS cylinders back into their original aligned states, recovering the initial anisotropy. This experiment demonstrates the potential of this system as a mechanically tunable photo luminescent polarizer.

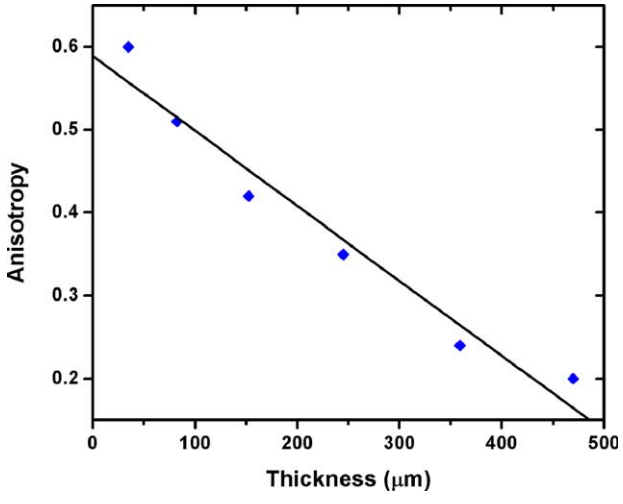

Fig. 5. Thickness dependence of anisotropy at 472 nm of a roll cast film. The excitation wavelength was ~400 nm and the thickness of the film varies between ~40 and ~470 μm. The variance in the anisotropy measured is ~10%.

3. Conclusion

We have investigated and characterized the alignment of a fluorescent conjugated polymer using a SIS triblock copolymer template. The guest PS-*g*-PPE molecules have similar orientational order to their host cylindrical polystyrene microdomains and can emit polarized light. Block copolymers offer a versatile approach for templating light emitting materials, not only fluorescent polymers, but also other nano-scale light emitting materials such as nanowires. The versatility of block copolymers also enables the modulation of light emission in different ways, for example, via photonic band gap manipulation with high molecular weight block copolymers [23,24], or as we demonstrated here, via mechanical deformation.

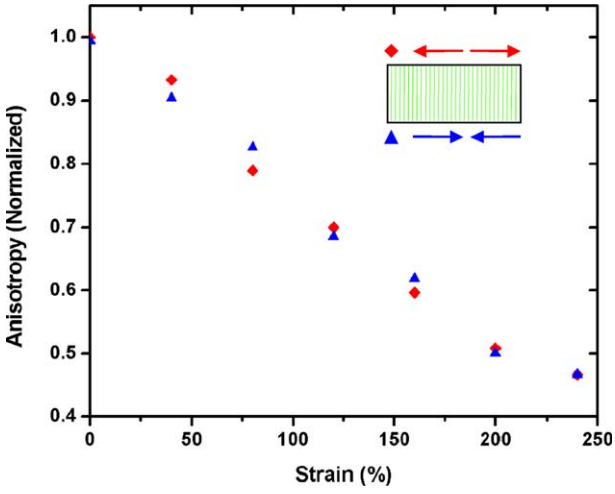

Fig. 6. Change of anisotropy with applied transverse strain. The film (~100 μm) was initially deformed to 240% and then released. The data shown is for the second loading/unloading cycle.

Acknowledgements

This research was supported by the US Army through the Institute for Soldier Nanotechnologies, under Contract DAAD-19-02-D-0002 with the US Army Research Office. The content does not necessarily reflect the position of the Government, and no official endorsement should be inferred.

References

[1] Sioula S, Hadjichristidis N, Thomas EL. Macromolecules 1998;31:5272.
[2] Folkes MJ, Keller A, Scalisi FP. Polymer 1971;12:793.
[3] De Rosa C, Park C, Thomas EL, Lotz B. Nature (London) 2000;405:433.
[4] Albalak RJ, Thomas EL. J Polym Sci, Part B: Polym Phys 1993;31:37.
[5] Morkved TL, Lu M, Urbas AM, Ehrichs EE, Jaeger HM, Mansky P, et al. Science (Washington, DC) 1996;273:931.
[6] Winter HH, Scott DB, Gronski W, Okamoto S, Hashimoto T. Macromolecules 1993;26:7236.
[7] Ha Y-H, Thomas EL. Macromolecules 2002;35:4419.
[8] Li RR, Dapkus PD, Thompson ME, Jeong WG, Harrison C, Chaikin PM, et al. Appl Phys Lett 2000;76:1689.
[9] Cheng JY, Ross CA, Chan VZH, Thomas EL, Lammertink RGH, Vancso GJ. Adv Mater 2001;13:1174.
[10] Park C, Yoon JS, Thomas EL. Polymer 2003;44:6725.
[11] Ha Y-H, Kwon Y, Breiner TE, Chan EP, Tzianetopoulou T, Cohen RE, et al. Macromolecules 2005;38:5170–5179.
[12] Bockstaller M, Michiewica R, Thomas EL. Adv Mater 2005;17:1331–1349.
[13] Park C, Yoon JS, Thomas EL. Polymer 2003;44:6725.
[14] Hamaguchi M, Yoshino K. Polym Adv Technol 1997;8:399.
[15] Hagler TW, Pakbaz K, Moulton J, Wudl F, Smith P, Heeger AJ. Polym Commun 1991;32:339.
[16] Smith RC, Fischer WM, Gin DL. J Am Chem Soc 1997;119:4092.
[17] Breen C, Deng T, Breiner T, Thomas EL, Swager TM. J Am Chem Soc 2003;125:9942.
[18] Honeker CC, Thomas EL, Albalak RJ, Hajduk DA, Gruner SM, Capel MC. Macromolecules 2000;33:9395.
[19] Honeker CC, Thomas EL. Macromolecules 2000;33:9407.
[20] Cotts PM, Swager TM, Zhou Q. Macromolecules 1996;29:7323.
[21] Note that this definition of r yields a nonzero value even for an isotropic film.
[22] Lakowicz JR. Principles of fluorescence spectroscopy. New York: Kluwer Academic Press; 1999.
[23] Fink Y, Urbas AM, Bawendi MG, Joannopoulos JD, Thomas EL. J Lightwave Technol 1999;17:1963.
[24] Edrington AC, Urbas AM, DeRege P, Chen CX, Swager TM, Hadjichristidis N, et al. Adv Mater 2001;13:421.